Biodegradable Comb-like Dendritic Tri-block Copolymer Promotes Nerve Cell Functions

Changhong Zhao[1],* Jiansheng Yu[1] and Meizhong Hu[1]

[1]Department of Pharmacy, Tongren Polytechnic College, Education Park of Tongren, Tongren 554300, China
*Email: ashuipp@163.com

Abstract

Novel symmetric biodegradable dendritic tri-block copolymer, consisting of a core of hydrophobic poly(L-lactide) (PLLA) block and 32 poly(L-lysine) (PLL) arms, was synthesized via a facile chemistry route. The as-synthesized tri-block copolymer was characterized with ^{1}H NMR, water contact angle measurements, GPC test, and DSC analysis. The ^{1}H NMR and GPC tests indicated that the tri-block copolymer, PLL-PLLA-PLL, with well-defined architecture was synthesized. The water contact angle measurements demonstrated that the incorporation of L-lysine improved prominently the hydrophilicity, and the DSC analysis indicated that the crystalline region of PLLA was slightly modified by the L-lysine component, decreasing melting temperature and crystallinity in the PLL-PLLA-PLL copolymer. NPCs and PC12 cells were seeded on PLLA, dendritic PLLA with 32 L-lysine terminals (d-PLLA-d), and PLL-PLLA-PLL films to investigate cell attachment, proliferation, and differentiation. The results strongly demonstrated that d-PLLA-d and PLL-PLLA-PLL films, especially PLL-PLLA-PLL films, dramatically promoted cell attachment, proliferation, and, more importantly, differentiation, particularly neurite outgrowth.

Keywords: dendritic tri-block copolymer, nerve cell functions, poly(L-lactide), poly(L-lysine)

Introduction

Even though the end-to-end surgical reconnection of nerve ends and autologous nerve graft has improved the clinic treatments for peripheral nervous system (PNS) and central nervous system (CNS) injuries, these treatments show some severe limitations. End-to-end reconnection has been demonstrated to be an effective modality for the treatment of nerve injuries with small gaps, but not for long gaps.[1] Autologous nerve graft has limited donor sources, leaving dysfunction in the donor site. Moreover, treatments for CNS are more challenging than for PNS due to the poor regeneration of CNS axons, glial scars, and slow macrophages infiltration. Thus, the advanced biomaterials to support nerve cell proliferation and neurite extension to grow across the lesion site and bridge the nerve gap are highly desired. Chemistry, topography, charges, and mechanical properties have been demonstrated to play important roles in governing cell adhesion, proliferation, and differentiation.[1-3] Positive charges can participate in cellular events, such as attachment, proliferation, differentiation, and nerve neurite extension.[4-9] Recently, cationic poly(L-lysine) (PLL) have been incorporated into biomaterials covalently or non-covalently to provide cell binding sites and positive charge for promoting cell functions due to the electrostatic interactions with the anion sites of cytoplasmic membranes.[7, 10-12]

Poly(L-lactide) (PLLA) as a biodegradable aliphatic polyester and its copolymers have been developed for applications in pharmaceutics and tissue engineering due to their low immunogenicity, excellent biocompatibility, and biodegradability.[13-17] On the other hand, they possess some fatal drawbacks which can be

exemplified as high hydrophobicity, poor cell affinity, and high crystallinity.[18] Consequently, it is important to develop approaches to modify PLLA properties and improve tissue engineering applications. To date, the attractive approaches developed include incorporation of hydrophilic components into PLLA backbone and synthesis of branched chemical structures. [19, 20]

In this study, we aim to develop a symmetric amphiphilic polycationic dendritic PLL-PLLA-PLL tri-block copolymer and investigate the functions of pheochromocytoma cells (PC12) and neural progenitor cells (NPCs) on this copolymer film. Recently, the synthesis of dendritic PLLA copolymers with the hydrophobic PLLA chain as the core has been reported. PLLA copolymer with two symmetric dendritic PLL was prepared to study its DNA binding affinity as gene carrier.[21] Amphiphilic PLLA-b-dendritic PLL was also synthesized with a metal-free catalyst.[22] However, the PLLA core had a low molecular weight of ~3000 g/mol due to the ring-opening polymerization (ROP) of L-lactide monomer initiated by a free hydroxyl group in organic solution. In addition, in both studies the PLL was obtained through dendritic structure of lysine instead of polymerization of L-Lysine monomers. In the present study, we will report a facile modality to synthesize symmetric amphiphilic dendritic PLL-PLLA-PLL tri-block copolymer with a high molecular weight, in which the PLL block will be synthesized via ROP reaction of L-Lysine monomers. The incorporation of cationic PLL into PLLA is expected to improve hydrophilicity and promote nerve cell functions including cell adhesion, proliferation, and differentiation. In addition, because of the presence of a high molecular PLLA core with certain mechanical properties, the copolymer might be a good candidate biomaterial for generating nerve conduit to guide nerve cell functions.

Experimental section

Synthesis of PLL-PLLA-PLL tri-block copolymer
PLLA with 32 amine terminal groups (d-PLLA-d, M_n = 62,533 g/mol; M_w = 80,042 g/mol) as shown in Figure 1A was synthesized as described

previously.[23] First, the PLLA was synthesized via ROP reaction of L-Lactide monomer initiated by propylene glycol to bear two hydroxyl groups. Then the hydroxyl terminals were converted into amine terminals by N-Boc-L-Glycine. ε-carbobenzyloxy-L-lysine (Z-L-Lys, 4 g, 14.3 mmol) was thoroughly dissolved in anhydrous THF (100 mL) at 50°C under stirring. Then Triphosgene (1.42 g, 4.78 mmol) dissolved in anhydrous THF (25 mL) was added to the above Z-L-Lys/THF solution dropwise and the reaction continued for 2 h under nitrogen gas protection.
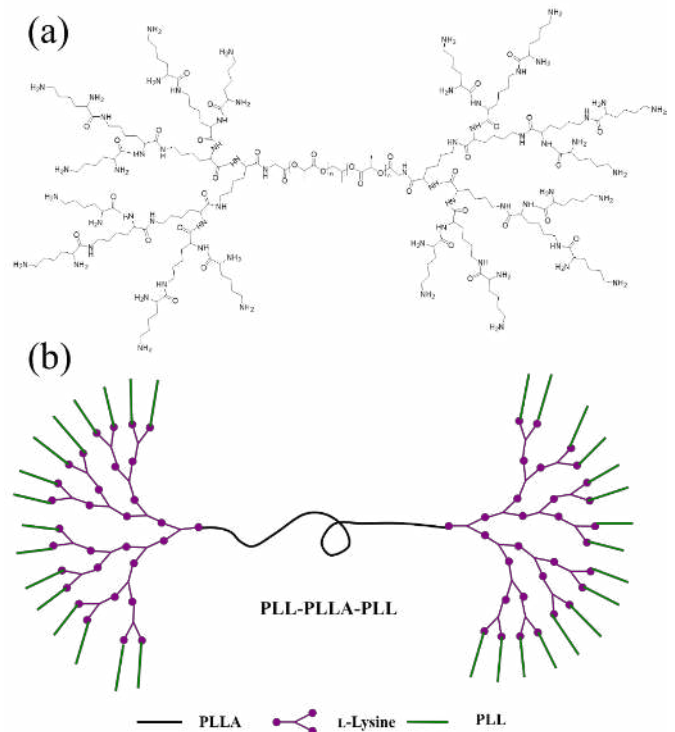

Figure 1. (a) Chemical structure of d-PLLA-d and (b) schematic structure of PLL-PLLA-PLL

After two precipitations in anhydrous hexane, the Z-L-Lys-N-carboxyanhydride (Z-L-Lys NCA) was completely dried under reduced pressure with a yield of ~88%. The d-PLLA-d with 32 amine terminal groups was used to initiate the polymerization of Z-L-Lys NCA in anhydrous DMF at 40°C for 4 days. After the DMF was removed in vacuum, the copolymer was deprotected with a 33 wt% hydrobromic acid solution in acetic acid for 1 h at room temperature. Eventually, the solution was precipitated twice in cold ethyl ether

and the copolymer was completely dried under reduced pressure. ^{1}H NMR (500 MHz, CDCl[3]): δ (ppm): 5.15 (q, 1H, -CH-), 4.30 (t, 1H, -CH-), 3.18 (t, 2H, -CH[2]-), 1.8 (t, 2H, -CH[2]-), 1.5 (t, 2H, -CH[2]-), 1.2 (t), 1.58 (q, 2H, -CH[3]). (Yield: 95%)

For cell studies, the polymers were hot-compressed into films between two clean glass slides. First, the polymer was melt at 190℃ and compressed between two glass slides. Then, the sample was cooled down to room temperature. The films were punched into disks with identical dimension (~1 × ~5 mm, thickness × diameter).

Characterization

^{1}H NMR spectra were recorded on a Bruker DRX-500 with CDCl[3] containing tetramethylsilane (TMS) as solvent. GPC measurements were performed on a Waters HPLC system equipped with a Model 2690D separation module, a Model 2410 refractive index detector, and Shodex columns. The linear polystyrene (PS) was used as standard to calculate molecular weights. Wettability for all films was analyzed on XG-7501B (Xuanyichuangxi Industrial Equipment, China). Fifteen μL of distilled water were dropped onto the film, and the photographs of water droplets were taken when droplets were stable. The water contact angle was measured from those images using ImageJ software (National Institutes of Health, Bethesda, MD). Differential scanning calorimetric (DSC) analysis was performed on a DSC2910 thermal analysis system (TA Instruments Inc., USA) at a heating rate of 20 ^{o}C/min under the protection of nitrogen atmosphere. The equation $\chi_c=(\Delta H_m-\Delta H_c)/\Delta H_m^0$ was used to calculate the crystallinity, in which the heats of fusion ΔH_m and ΔH_c were obtained from the melting endothermal and crystallization exothermal peaks of DSC curves and the heat of fusion for 100% crystalline PLLA; ΔHm^0 = 93.6 J/g was obtained from literatures.[18] Tensile properties were determined on a dynamic mechanical analyzer (DMTA-5, Rheometric Scientific) at 37°C. Polymer strips (~21 × ~1.5 × ~0.5 mm, length × width × thickness) were pulled at a strain rate of 0.0002 s^{-1}. Five specimens were run for each polymer and elastic (E) modulus was calculated from the initial slope of the stress-strain curve.

NPC cell attachment, proliferation, and differentiation

Polymer films were sterilized according to previous protocols,[9, 24-29] Briefly, the films were washed with 70% ethanol solution twice to remove dust, immersed in 70% ethanol solution for 30 min, and then exposed to UV light for 20 min. NPCs were seeded onto the films at a density of ~12000 cells/cm^{2} in 24-well tissue culture plates with serum-free growth media containing DMEM/F12 medium (Invitrogen, Carlsbad, CA), 20 ng/mL basic fibroblastic growth factor (bFGF, Invitrogen), 20 ng/mL recombinant human epidermal growth factor (EGF, Invitrogen), 1% GlutaMAX (Invitrogen), and 1% penicillin/streptomycin (Invitrogen). The NPCs were cultured for 4 h, 1, 4, and 7 days to investigate cell attachment and proliferation. At each time point, the cell numbers were quantified with an MTT assay according to the manufacturer's manual. To visualize NPCs, they were fixed with 4% paraformaldehyde (PFA) solution at room temperature for ~30 min, followed by washing with PBS twice before stained with 4', 6'-diamidino-2-phenylindole (DAPI). The DAPI-stained cells were photographed with confocal laser scanning microscopy (LEICA TCS SD2, Germany). To confirm that cells were still undifferentiated at day 7, the fixed cells were blocked with PBS solution containing 0.3% Triton X-100 and 1% bovine serum albumin (BSA) for ~30 min. Further, NPCs were incubated with mouse monoclonal anti-nestin (1:500, v/v) at 37°C for 1 h and subsequently at 4°C overnight. Afterwards, NPCs were rinsed with PBS containing 1% BSA thoroughly prior to staining with goat anti-mouse IgG-FITC (1:100, v/v) at 37°C for 2 h, followed by staining with DAPI at room temperature. NPCs were observed using confocal laser scanning microscopy. NPCs in ~50 images were counted to determine the percentage of nestin-positive cells on the total cell number.

To evaluate NPC differentiation on PLLA, d-PLLA-d, and PLL-PLLA-PLL films, NPCs were seeded on those films at a density of ~5000 cells/cm^{2} with growth medium. At 12 h post-seeding, the growth medium was substituted with a differentiation medium containing DMEM/F12, GlutaMAX (1%),

fetal bovine serum (1%), and penicillin/streptomycin (1%). The cell culture continued for 7 days, during which the differentiation medium was refreshed every other day. Afterwards, the NPCs were fixed and blocked using the same protocol for nestin staining. Rabbit monoclonal anti-neurofilament 200 (NF), rabbit monoclonal anti-glial fibrillary acidic protein (GFAP), mouse monoclonal anti-β-tubulin III, mouse monoclonal anti-oligodendrocyte marker O4 were employed to stain mature neurons, astrocytes, immature neurons, and oligodendrocytes, respectively. Then NPCs were further labeled with goat anti-mouse IgG-FITC for β-tubulin III and O4 and CF647 goat anti-rabbit IgG for NF and GFAP. The immunostained NPCs were stained with DAPI to visualize nuclei prior to observation using the confocal laser scanning microscopy.

PC12 cell attachment, proliferation, and differentiation

Prior to cell culture, PLLA, d-PLLA-d, and PLL-PLLA-PLL films were sterilized as described previously.[25, 26, 30] Rat PC12 cells (CRL-1721, ATCC, Manassas, VA) were seeded on films at a density of ~13000 cells/cm^2 in 24-well tissue culture plates with a growth medium containing F-12K medium (Gibco, Grand Island, NY), 15% horse serum, 5% fetal bovine serum (FBS, Gibco), and 1% penicillin/streptomycin (Gibco) in a cell incubator. The PC12 cells were cultured for 4 h, 1, 4, and 7 days and the cell numbers were quantified with a MTT assay to evaluate cell attachment and proliferation.

To study PC12 cell differentiation on those films, cells were cultured with a growth medium containing 50 ng/mL NGF for 7 days. Afterwards, the culture medium was discarded, and PC12 cells were rinsed twice with PBS. Cells were fixed with 4% PFA solution for ~15 min, rinsed with PBS solution twice, and permeabilized with 0.2% Triton X-100 solution. Subsequently, the cells were stained with rhodamine-phalloidin (RP) for 1 h at 37°C and with DAPI at room temperature. Confocal laser scanning microscopy was employed to photograph the stained PC12 cells.

Statistical analysis

All studies were performed in quadruplicates for each group. Each value was written as mean ± standard deviation. The data were analyzed with the Student's t-test, assuming statistical significance at $p < 0.05$ or $p < 0.01$ between two groups.

Results and discussion

Synthesis of PLL-PLLA-PLL

A dendritic d-PLLA-d with 32 amine groups as shown in Figure 1A was used to initiate the ROP reaction of Z-L-Lys NCA and the as-synthesized PLL-PLLA-PLL amphiphilic tri-block copolymer had 32 PLL blocks as shown in schematic Figure 1B. To confirm the chemical structure, ^{1}H NMR spectra of PLL-PLLA-PLL copolymer was recorded with CDCl$_3$ as solvent (Figure 2). The chemical shifts of the PLLA block came up at 1.58 ppm and 5.15 ppm, which were assigned to -CH$_3$ and -CH-, respectively. The chemical shifts of PLL blocks at **a** and **b** were assigned to -CH- and -CH$_2$- near to the -NH$_2$ end group (Figure 2), respectively. The other chemical shifts (**c**, **d**, and **e**) of the PLL block partly overlapped with the peak of PLLA block at 1.58 ppm. These ^{1}H NMR results are in accordance with previous findings. [21, 22, 31]
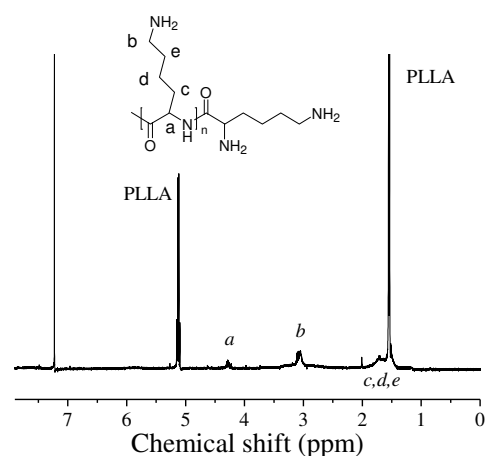

Figure 2. ^{1}H NMR spectra of PLL-PLLA-PLL tri-block copolymer

Characterization

GPC measurements were employed to determine the molecular weights of PLLA, d-PLLA-d, and PLL-

PLLA-PLL polymers as shown in Table 1. The number-averaged molecular weight increased from 62,533 g/mol for PLLA to 66,192 g/mol for d-PLLA-d, which was close to the $M_{n,NMR}$ (66,211 g/mol) and $M_{n,theoretic}$ (66,381 g/mol). The deviation of the GPC molecular weight from the molecular weights calculated from ^{1}H NMR and feed ratio should be attributed to the fact that the GPC molecular weights were calibrated and calculated from linear PS standard, whereas d-PLLA-d possessed a dendritic structure. In addition, the PDI also increased from 1.28 for PLLA to 1.32 for d-PLLA-d, due to the architecture change from a linear chain to a dendritic chain.

Similarly, the occurrence of polymerization of L-Lysine monomer initiated by d-PLLA-d caused the increase of number-averaged molecular weight from 66,192 g/mol for d-PLLA-d to 90,213 g/mol for PLL-PLLA-PLL, whwreas the PDI increased to 1.45 and the $M_{n,GPC}$ was significantly lower than the $M_{n,theoretic}$ of 93,127 g/mol. On the other hand, the $M_{n,NMR}$ of PLL-PLLA-PLL was calculated from ^{1}H NMR spectra to be 92,879 g/mol, which was nearly identical to the $M_{n,theoretic}$ of 93,127 g/mol. These results indicated that the L-Lysine monomer was completely consumed during polymerization of L-Lysine monomer, and the architecture of tri-block copolymer was confirmed.

Table 1. Molecular weights, water contact angles, and thermal properties of PLLA, d-PLLA-d, and PLL-PLLA-PLL

Polymers	$M_{n,GPC}$[a]	$M_{w,GPC}$[a]	M_w/M_n[a]	$M_{n,NMR}$[b]	$M_{n,theoretic}$[c]	Water contact angle (°)	T_m (℃)	χ_c (%)
PLLA	62,533	80,042	1.28			76 ± 4	158	22
d-PLLA-d	66,192	87,373	1.32	66,211	66,381	65 ± 6	152	17
PLL-PLLA-PLL	90,213	130,809	1.45	92,879	93,127	51 ± 5	141	9

[a] Obtained from GPC test
[b] Calculated from ^{1}H NMR spectrum.
[c] Calculated from the feed ratio.

The wettability can be influenced by chemistry.[25, 26] As shown in Table 1, the incorporation of L-Lysine improved the hydrophilicity. The water contact angles decreased from 76 ± 4 ° on PLLA films to 65 ± 6 ° and 51 ± 5 ° on d-PLLA-d and PLL-PLLA-PLL films, respectively. The thermal properties were determined by DSC test as shown in Table 1. The melting temperature decreased increasing the composition of L-Lysine in the polymer, and the crystallinity also decreased dramatically from 22% in PLLA films to 17% and 9% in d-PLLA-d and PLL-PLLA-PLL films, respectively. The incorporation of L-Lysine into PLLA might have altered the PLLA crystalline region, lowering the melting point and crystallinity.

Cell attachment and proliferation
After generating disks of these polymers, NPCs and PC12 cells were seeded on these disks to investigate cell functions. Cell attachment and proliferation of NPCs and PC12 cells are shown in Figure 3. NPCs were cultured in serum-free medium to exclude the effect of serum protein on cell functions. Figure 3A shows the fluorescent images of NPC proliferation at day 1, 4, and 7. Clearly, the number of NPCs increased with the time of culture. In addition, NPCs presented the highest density on PLL-PLLA-PLL films, whereas the lowest proliferation was observed on PLLA films. On the other hand, more neurospheres were found on d-PLLA-d and PLL-PLLA-PLL films, especially PLL-PLLA-PLL films, indicating that PLL-PLLA-PLL were optimal for NPC proliferation. NPC attachment and proliferation, represented by cell numbers, were also quantified with a MTT assay (Figure 3C). At 4 h, PLL-PLLA-PLL films showed significantly better cell attachment than PLLA. From day 1, the proliferation on d-PLLA-d films started to be significantly faster than on PLLA ones and, however, remarkably slower than on

PLL-PLLA-PLL, which agreed with the observation in Figure 3A. Similarly, PC12 cells showed the highest density on PLL-PLLA-PLL films and the lowest density on PLLA films at day 1, 4, and 7, as indicated in Figure 3B. Again, the PLL-PLLA-PLL films showed significantly higher cell attachment than PLLA ones at 4 h. From day 1, the proliferation on d-PLLA-d films started to be faster than on PLLA ones, but remarkably slower than on PLL-PLLA-PLL ones.
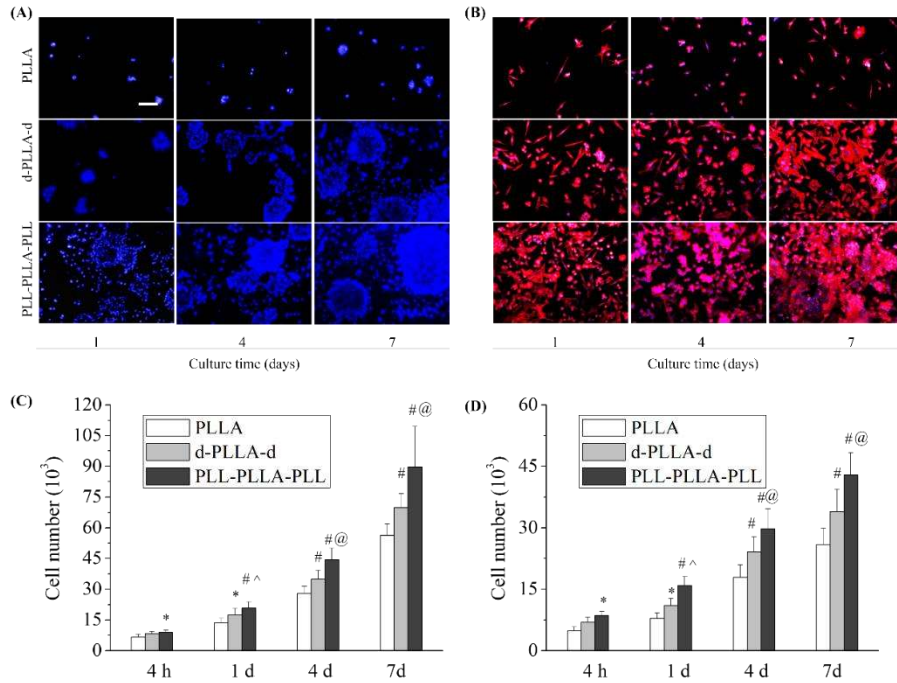

Figure 3. (A) Fluorescent images of NPC neurospheres stained with DAPI (blue) at day 1, 4, and 7 on PLLA, d-PLLA-d, and PLL-PLLA-PLL films. Scale bar of 50 μm. (B) Fluorescent images of PC12 cells stained with RP (red) and DAPI (blue) at day 1, 4, and 7 on PLLA, d-PLLA-d, and PLL-PLLA-PLL films. Scale bar of 50 μm. (C) NPC cell proliferation represented by cell numbers determined by MTT assay at 4 h, day 1, 2, and 4. (D) PC12 cell proliferation represented by cell numbers determined by MTT assay at 4 h, day 1, 2, and 4. *: $p < 0.05$ and #: $p < 0.01$ relative to PLLA films; ^: $p < 0.05$ and @: $p < 0.01$ relative to d-PLLA-d films.

The main factors, in this study, involved in cell response included hydrophilicity, charges, and mechanical properties. The introduction of L-Lysine monomers influenced the hydrophilicity of PLLA polymer due to the hydrophilic nature of L-Lysine. The water contact angles on PLLA, d-PLLA-d, and PLL-PLLA-PLL films decreased from 68.2 ± 1.6° on PLLA films to 59.7 ± 2.7° and 45.1 ± 5.9° on d-PLLA-d and PLL-PLLA-PLL films, respectively. Due to the fact that hydrophobic surfaces induce adsorption of nonadhesive proteins and denaturation of adhesive proteins, whereas hydrophilic surfaces have low protein binding, the substrate surfaces with an intermediate energy and a water contact angle of ~50° have been demonstrated to support better cell attachment and proliferation than those hydrophobic or hydrophilic.[32] The charges provided by L-Lysine monomers played a critical role in early cellular events including attachment and proliferation through the strong electrostatic interactions with the anion sites of cytoplasmic membrane.[7, 10, 21] Even though the charge density was not determined, it is reasonable to consider the charge density in the order of PLL-PLLA-PLL > d-PLLA-d > PLLA according to the composition of L-Lysine in PLLA polymer. Hence, cell attachment and proliferation were promoted in the same order. Earlier findings suggested that the 2~3 wt% PLL in PEG hydrogel induced optimal NPC

functions, such as attachment, proliferation, and neurite extension. [33]However, the mass compositions of L-Lysine in d-PLLA-d and PLL-PLLA-PLL in our study were calculated according to the molecular weights determined by GPC test to be ~5 wt% and ~30 wt%, respectively. Clearly, the PLL composition in PLL-PLLA-PLL films was higher than 2~3 wt% and induced the best NPC attachment and proliferation. Note that the d-PLLA-d and PLL-PLLA-PLL films in our study were hard substrata instead of soft hydrogesl. Consequently, the real charge distribution on the d-PLLA-d and PLL-PLLA-PLL film surfaces might be different from that in hydrogels, which caused different response for NPCs. The mechanical properties might also influence attachment and differentiation of NPCs and PC12 cells. It has been demonstrated that neural stem cells (NSCs) proliferated well on substrata with a brain-tissue-like elastic modulus (E) of ~3.5 kPa and PC12 cells on softer materials.[31, 34, 35] The E values of PLLA, d-PLLA-d, and PLL-PLLA-PLL films were measured to be 479 ± 58, 386 ± 35, and 179 ± 41 MPa, respectively. With the increase of L-Lysine composition, the polymer tended to be softer, which might partly explain the better PC12 cell attachment and proliferation on d-PLLA-d films and especially PLL-PLLA-PLL films compared with harder PLLA films. In addition, the NPCs responded to higher E values of 179-479 MPa, which is a range comparable to nerve conduit materials. The role of mechanical properties in cell–material interactions functioned through pathways involving mechanotransduction and integrin-mediated focal adhesion.[2, 6, 34, 35] As a result, the integration of hydrophilicity, charges, and mechanical properties supported better cell attachment and proliferation on d-PLLA-d and PLL-PLLA-PLLA films than on PLLA ones.

Cell differentiation

The incorporation of L-Lysine into PLLA influenced the differentiation of NPCs and PC12 cells as depicted in Figure 4. Primary CNS lineages, neurons, astrocytes, and oligodendrocytes, differentiated from NPCs on PLLA, d-PLLA-d, and PLL-PLLA-PLL films were immunostained as shown in Figure 4A. NPCs displayed best neurite outgrowth, stained with mature neural marker NF, on PLL-PLLA-PLL films; however, the lowest neurite outgrowth on PLLA ones. Likewise, the immature neurons stained with anti-β-tubulin III and astrocytes stained with anti-GFAP grew dramatically better on PLL-PLLA-PLL films than on the others. On the other hand, NPCs stained with oligodendrocyte marker O4 did not show significant difference between d-PLLA-d and PLL-PLLA-PLL films, even though better than PLLA ones. The d-PLLA-d and PLL-PLLA-PLL films, especially PLL-PLLA-PLL ones, also promoted neurite outgrowth of PC12 cells, as indicated in Figure 4B. PC12 cells on d-PLLA-d films projected more neurites from cell bodies than on PLLA ones, and the neurite outgrowth was even better on PLL-PLLA-PLL films than on d-PLLA-d ones.

To further analyze NPC differentiation on PLLA, d-PLLA-d, and PLL-PLLA-PLL films, the total percentage of differentiated NPCs, total differentiated NPCs divided by the total cell number, and the percentages of NPCs differentiated into neurons, astrocytes, and oligodendrocytes, defined as antibody-positive NPCs divided by the total cell number, were quantified from ~70 fluorescent images using ImageJ software, as shown in Figure 5. The NPC differentiation percentage on PLLA films was 26 ± 5%, whereas it increased to 59 ± 17% and 98 ± 10% on d-PLLA-d and PLL-PLLA-PLL films, respectively. Similarly, the percentages of neuron differentiation on PLLA, d-PLLA-d, and PLL-PLLA-PLL films were calculated to be 14 ± 4%, 31 ± 8%, and 45 ± 11%, respectively. The same trend was observed for astrocytes and oligodendrocytes as demonstrated in Figure 5C and Figure 5D, respectively. Moreover, the neurite was also quantified from ~60 NF-immunostained images in terms of the percentage of cells bearing neurites, the number of neurites per cell, and the average neurite length using ImageJ software, as shown in Figure 5E-G. The percentages of NPCs bearing neurites on PLLA, d-PLLA-d, and PLL-PLLA-PLL films were calculated to be 15 ± 6%, 35 ± 6%, and 47 ± 8%, respectively. Consistently, the number of neurites per cell on PLL-PLLA-PLL was higher than on PLLA and d-PLLA-d films, especially PLLA films. The further measurement of average neurite length also demonstrated the same trend; NPCs

on PLL-PLLA-PLL films had the longest neurite outgrowth, whereas PLLA films supported the shortest neurite outgrowth (Figure 5G). These analyses strongly demonstrated that d-PLLA-d and especially PLL-PLLA-PLL films effectively strengthened NPC differentiation into neurons.
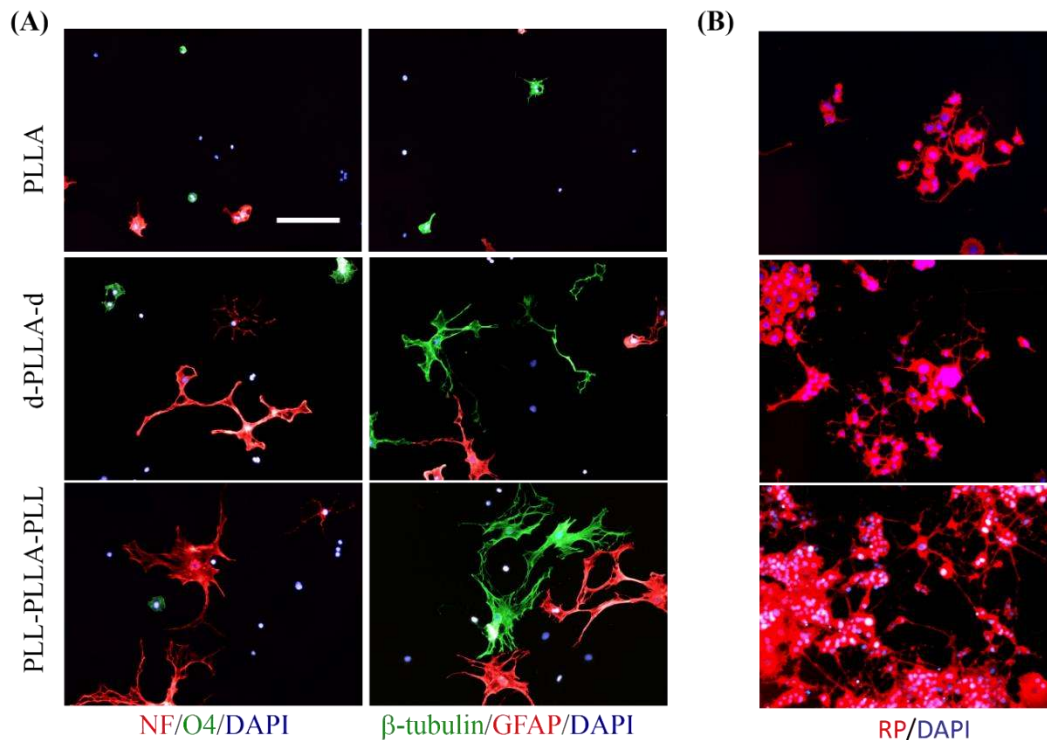

Figure 4. (A) Fluorescent images of differentiated NPCs on PLLA, d-PLLA-d, and PLL-PLLA-PLL films. The differentiated cells were immunostained with anti-NF (red, mature neurons), anti-O4 (green, oligodendrocytes), anti-β-tubulin III (green, immature neurons), anti-GFAP (red, astrocytes), and DAPI (blue, nuclei). Scale bar of 50 μm. (B) Fluorescent images of PC12 cells stained with RP (red) and DAPI (blue) after exposure to NGF for 7 days on PLLA, d-PLLA-d, and PLL-PLLA-PLL films. Scale bar of 100 μm.

The neurite outgrowth of PC12 cells in terms of the percentage of differentiated PC12 cells, number of neurites per cell, and neurite length on PLLA, d-PLLA-d, and PLL-PLLA-PLL films, when the PC12 cells were cultured in the presence of NGF at day 7, was also analyzed from ~70 RP-stained fluorescent images (Figure 5H-J) using ImageJ software. Similar to the results for NPC differentiation, the neurite outgrowth of PC12 cells was significantly stimulated on d-PLLA-d and PLL-PLLA-PLL films, and the PLL-PLLA-PLL films induced the best neurite outgrowth compared with PLLA and d-PLLA-d films.

Those results demonstrated the integrative roles of positive charges and mechanical properties in fostering NPC and PC12 cell differentiation. The promoted neurite extension by positive charges may associate with protein conformation changes, protein synthesis, redistribution of cell-membrane growth factors and adhesion ligands.[36] The dorsal root ganglion (DRG) neurites showed enhanced outgrowth on positively charged hydrogels.[6] The potential for PLL to induce efficient neural tissue differentiation of embryonic brain cells through interactions between PLL polycations and cell surfaces was also reported earlier.[37] Similarly, in this study the positive charges provided by L-Lysine monomers played an important role in stimulating neurite outgrowth in both NPCs and PC12 cells. Moreover, cell differentiation might be also affected by mechanical properties. NSCs

were found to have a higher number of neurons on softer gels, whereas have a lower number of glial cultures on harder gels.[34] The softer PLL-

PLLA-PLL films might favor neurite outgrowth compared with harder PLLA and PLLA-d films.
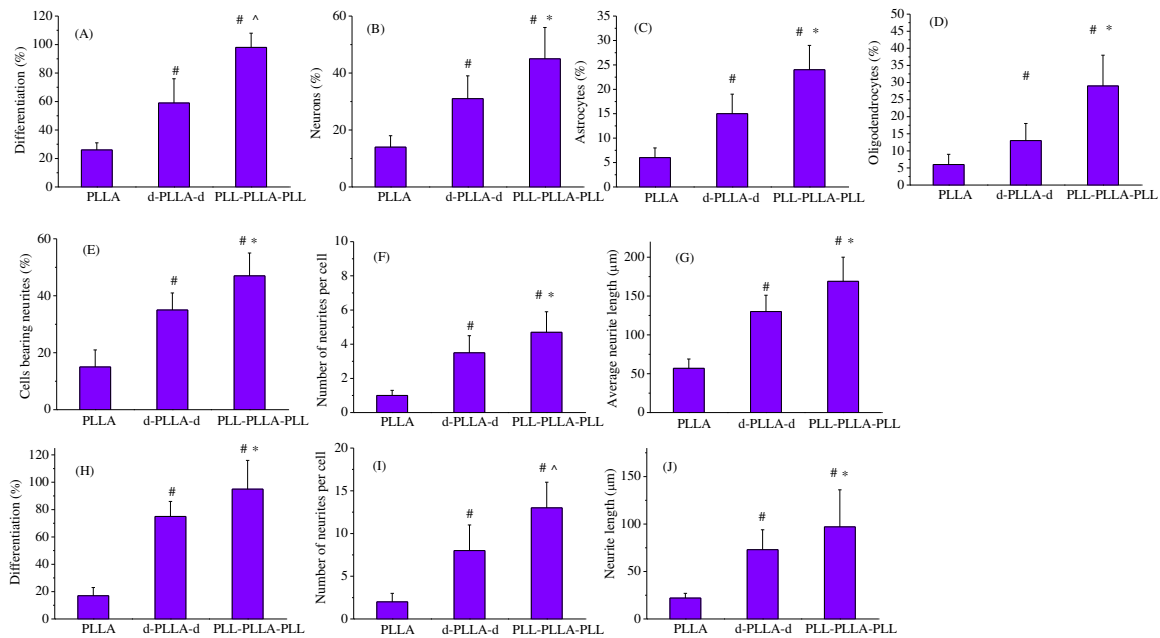

Figure 5. Percentage of (A) differentiated NPCs, (B) neurons (NF-positive), (C) astrocytes (GFAP-positive), and (D) oligodendrocytes (O4-positive) on PLLA, d-PLLA-d, and PLL-PLLA-PLL films. (E) Percentage of NPCs bearing neurites. (F) Number of neurites per cell. (G) Average neurite length. Quantification of differentiated PC12 cells. (H) Percentage of differentiated PC12 cells. (I) Average neurites per cell. (J) Neurite length. (A-D): *: $p < 0.01$ and #: $p < 0.01$ relative to PLLA and d-PLLA-d films, respectively. (D-G): *: $p < 0.05$ and #: $p < 0.01$ relative to d-PLLA-d and PLLA films, respectively. (H-J): #: $p < 0.01$ relative to PLLA films; *: $p < 0.05$ and ^: $p < 0.01$ relative to d-PLLA-d films.

Conclusion

A simple modality was utilized to synthesize symmetric biodegradable dendritic PLL-PLLA-PLL tri-block copolymer with a core of hydrophobic PLLA and dendritic PLL arms. NPCs and PC12 cells were seeded on PLLA, d-PLLA-d, and PLL-PLLA-PLL films. The results consistently demonstrated that d-PLLA-d and PLL-PLLA-PLL films, especially PLL-PLLA-PLL ones, dramatically promoted the differentiation nerve cells, particularly neurite outgrowth. Undoubtedly, PLL-PLLA-PLL tri-block copolymer might be used as a nerve conduit material.

Acknowledgments

References

1. Hoffman-Kim, D.; Mitchel, J. A.; Bellamkonda, R. V., Topography, Cell Response, and Neve Regeneration. In Annual Review of Biomedical Engineering, Vol 12, Yarmush, M. L.; Duncan, J. S.; Gray, M. L., Eds. Annual Reviews: Palo Alto, 2010; Vol. 12, pp 203-231.

2. Discher, D. E.; Janmey, P.; Wang, Y. L., Tissue cells feel and respond to the stiffness of their substrate. Science 2005, 310, 1139-1143.
http://dx.doi.org/10.1126/science.1116995
PMid:16293750

3. Yu, L. M. Y.; Leipzig, N. D.; Shoichet, M. S., Promoting neuron adhesion and growth. Materials Today 2008, 11, 36-43.
http://dx.doi.org/10.1016/S1369-7021(08)70088-9

4. Schneider, G. B.; English, A.; Abraham, M.; Zaharias, R.; Stanford, C.; Keller, J., The effect of hydrogel charge density on cell attachment. Biomaterials 2004, 25, 3023-3028.
http://dx.doi.org/10.1016/j.biomaterials.2003.09.084
PMid:14967535

5. Chen, Y. M.; Ogawa, R.; Kakugo, A.; Osada, Y.; Gong, J. P., Dynamic cell behavior on synthetic hydrogels with different charge densities. Soft Matter 2009, 5, 1804-1811.
http://dx.doi.org/10.1039/b818586g

6. Dadsetan, M.; Knight, A. M.; Lu, L. C.; Windebank, A. J.; Yaszemski, M. J., Stimulation of neurite outgrowth using positively charged hydrogels. Biomaterials 2009, 30, 3874-3881.
http://dx.doi.org/10.1016/j.biomaterials.2009.04.018
PMid:19427689 PMCid:PMC2716054

7. Rao, S. S.; Han, N.; Winter, J. O., Polylysine-Modified PEG-Based Hydrogels to Enhance the Neuro-Electrode Interface. Journal of Biomaterials Science-Polymer Edition 2011, 22, 611-625.
http://dx.doi.org/10.1163/092050610X488241
PMid:20566048

8. Wu, X., Progress in Mediating Cell Functions on Honeycomb Substratum. Journal of Postdoctoral Research April 2014, 1, 17.

9. Wu, X.; Wang, S., Biomimetic Calcium Carbonate Concentric Microgrooves with Tunable Widths for Promoting MC3T3-E1 Cell Functions. Advanced healthcare materials 2013, 2, 326-333.

10. Hynes, S. R.; McGregor, L. M.; Rauch, M. F.; Lavik, E. B., Photopolymerized poly(ethylene glycol)/poly(L-lysine) hydrogels for the delivery of neural progenitor cells. Journal of Biomaterials Science-Polymer Edition 2007, 18, 1017-1030.
http://dx.doi.org/10.1163/156856207781494368
PMid:17705996

11. Wang, J. H.; Hung, C. H.; Young, T. H., Proliferation and differentiation of neural stem cells on lysine-alanine sequential polymer substrates. Biomaterials 2006, 27, 3441-3450.
http://dx.doi.org/10.1016/j.biomaterials.2006.02.002
PMid:16516286

12. Wu, X.; Ye, L.; Liu, K.; Wang, W.; Wei, J.; Chen, F.; Liu, C., Antibacterial properties of mesoporous copper-doped silica xerogels. Biomedical Materials 2009, 4, 045008.
http://dx.doi.org/10.1088/1748-6041/4/4/045008
PMid:19605960

13. Yang, Y.; Bajaj, N.; Xu, P.; Ohn, K.; Tsifansky, M. D.; Yeo, Y., Development of highly porous large PLGA microparticles for pulmonary drug delivery. Biomaterials 2009, 30, 1947-1953.
http://dx.doi.org/10.1016/j.biomaterials.2008.12.044
PMid:19135245

14. Nasongkla, N.; Shuai, X.; Ai, H.; Weinberg, B. D.; Pink, J.; Boothman, D. A.; Gao, J. M., cRGD-functionalized polymer micelles for targeted doxorubicin delivery. Angew. Chem.-Int. Edit. 2004, 43, 6323-6327.
http://dx.doi.org/10.1002/anie.200460800
PMid:15558662

15. Ouchi, T.; Toyohara, M.; Arimura, H.; Ohya, Y., Preparation of poly(L-lactide)-based microspheres having a cationic or anionic surface using biodegradable surfactants. Biomacromolecules 2002, 3, 885-888.
http://dx.doi.org/10.1021/bm0200231
PMid:12217030

16. Deng, C.; Tian, H. Y.; Zhang, P. B.; Sun, J.; Chen, X. S.; Jing, X. B., Synthesis and characterization of RGD peptide grafted

poly(ethylene glycol)-b-poly(L-lactide)-b-poly(L-glutamic acid) triblock copolymer. Biomacromolecules 2006, 7, 590-596.
http://dx.doi.org/10.1021/bm050678c
PMid:16471935

17. Wei, J.; Lu, J.; Yan, Y.; Li, H.; Ma, J.; Wu, X.; Dai, C.; Liu, C., Preparation and characterization of well ordered mesoporous diopside nanobiomaterial. Journal of nanoscience and nanotechnology 2011, 11, 10746-10749.
http://dx.doi.org/10.1166/jnn.2011.3940
PMid:22408987

18. Gong, F. R.; Cheng, X. Y.; Wang, S. F.; Wang, Y.; Gao, Y.; Cheng, S. J., Biodegradable comb-dendritic tri-block copolymers consisting of poly(ethylene glycol) and poly(L-lactide): Synthesis, characterizations, and regulation of surface morphology and cell responses. Polymer 2009, 50, 2775-2785.
http://dx.doi.org/10.1016/j.polymer.2009.04.033

19. Cai, Q.; Zhao, Y. L.; Bei, J. Z.; Xi, F.; Wang, S. G., Synthesis and properties of star-shaped polylactide attached to poly(amidoamine) dendrimer. Biomacromolecules 2003, 4, 828-834.
http://dx.doi.org/10.1021/bm034051a
PMid:12741805

20. Chen, H. T.; Neerman, M. F.; Parrish, A. R.; Simanek, E. E., Cytotoxicity, hemolysis, and acute in vivo toxicity of dendrimers based on melamine, candidate vehicles for drug delivery. Journal of the American Chemical Society 2004, 126, 10044-10048.
http://dx.doi.org/10.1021/ja048548j
PMid:15303879

21. Li, Y.; Cui, L.; Li, Q. B.; Jia, L.; Xu, Y. H.; Fang, Q.; Cao, A., Novel symmetric amphiphilic dendritic poly(L-lysine)-b-poly(L-lactide)-b-dendritic poly(L-lysine) with high plasmid DNA binding affinity as a biodegradable gene carrier. Biomacromolecules 2007, 8, 1409-1416.
http://dx.doi.org/10.1021/bm0701806
PMid:17458996

22. Li, Y.; Li, Q. B.; Li, F. X.; Zhang, H. Y.; Jia, L.; Yu, J. Y.; Fang, Q.; Cao, A., Amphiphilic poly(L-lactide)-b-dendritic poly(L-lysine)s synthesized with a metal-free catalyst and new dendron initiators: Chemical preparation and characterization. Biomacromolecules 2006, 7, 224-231.
http://dx.doi.org/10.1021/bm050602g
PMid:16398519

23. Chapman, T. M.; Hillyer, G. L.; Mahan, E. J.; Shaffer, K. A., HYDRAAMPHIPHILES - NOVEL LINEAR DENDRITIC BLOCK-COPOLYMER SURFACTANTS. Journal of the American Chemical Society 1994, 116, 11195-11196.
http://dx.doi.org/10.1021/ja00103a060

24. Wei, J.; Wu, X.; Liu, C.; Jia, J.; Heo, S. j.; Kim, S. e.; Hyun, Y. t.; Shin, J. W., Fabrication of Bioactive Scaffold of Poly (ε-Caprolactone) and Nanofiber Wollastonite Composite. Journal of the American Ceramic Society 2009, 92, 1017-1023.
http://dx.doi.org/10.1111/j.1551-2916.2009.03002.x

25. Wu, X.; Wang, S., Regulating MC3T3-E1 Cells on Deformable Poly (ε-caprolactone) Honeycomb Films Prepared Using a Surfactant-Free Breath Figure Method in a Water-Miscible Solvent. ACS applied materials & interfaces 2012, 4, 4966-4975.
http://dx.doi.org/10.1021/am301334s
PMid:22889037

26. Wu, X.; Wang, S., Integration of photo-crosslinking and breath figures to fabricate biodegradable polymer substrates with tunable pores that regulate cellular behavior. Polymer 2014, 55, 1756-1762.
http://dx.doi.org/10.1016/j.polymer.2014.02.029

27. Wu, X.; Wei, J.; Lu, X.; Lv, Y.; Chen, F.; Zhang, Y.; Liu, C., Chemical characteristics and hemostatic performances of ordered mesoporous calcium-doped silica xerogels. Biomedical Materials 2010, 5, 035006.
http://dx.doi.org/10.1088/1748-6041/5/3/035006
PMid:20460688

28. Zhou, H.; Wei, J.; Wu, X.; Shi, J.; Liu, C.; Jia, J.; Dai, C.; Gan, Q., The bio-functional role of calcium in mesoporous silica xerogels on the responses of osteoblasts in vitro. Journal of Materials Science: Materials in Medicine 2010, 21, 2175-2185.

http://dx.doi.org/10.1007/s10856-010-4083-8
PMid:20411307

29. Zhou, H.; Wu, X.; Wei, J.; Lu, X.; Zhang, S.; Shi, J.; Liu, C., Stimulated osteoblastic proliferation by mesoporous silica xerogel with high specific surface area. Journal of Materials Science: Materials in Medicine 2011, 22, 731-739.
http://dx.doi.org/10.1007/s10856-011-4239-1
PMid:21287245

30. Wu, X. H.; Wu, Z. Y.; Su, J. C.; Yan, Y. G.; Yu, B. Q.; Wei, J.; Zhao, L. M., Nano-hydroxyapatite promotes self-assembly of honeycomb pores in poly(l-lactide) films through breath-figure method and MC3T3-E1 cell functions. RSC Advances 2015, 5, 6607-6616.
http://dx.doi.org/10.1039/C4RA13843K

31. Cai, L.; Lu, J.; Sheen, V.; Wang, S. F., Promoting Nerve Cell Functions on Hydrogels Grafted with Poly(L-lysine).
Biomacromolecules 2012, 13, 342-349.
http://dx.doi.org/10.1021/bm300381d
http://dx.doi.org/10.1021/bm201763n
PMid:22251248 PMCid:PMC3538025

32. Cai, L.; Wang, K.; Wang, S., Poly(ethylene glycol)-grafted poly(propylene fumarate) networks and parabolic dependence of MC3T3 cell behavior on the network composition. Biomaterials 2010, 31, 4457-4466.
http://dx.doi.org/10.1016/j.biomaterials.2010.02.020
PMid:20202682

33. Cai, L.; Lu, J.; Sheen, V.; Wang, S. F., Optimal Poly(L-lysine) Grafting Density in Hydrogels for Promoting Neural Progenitor Cell Functions. Biomacromolecules 2012, 13, 1663-1674.
http://dx.doi.org/10.1021/bm300381d
http://dx.doi.org/10.1021/bm201763n

34. Saha, K.; Keung, A. J.; Irwin, E. F.; Li, Y.; Little, L.; Schaffer, D. V.; Healy, K. E., Substrate Modulus Directs Neural Stem Cell Behavior. Biophysical Journal 2008, 95, 4426-4438.
http://dx.doi.org/10.1529/biophysj.108.132217
PMid:18658232 PMCid:PMC2567955

35. Leipzig, N. D.; Shoichet, M. S., The effect of substrate stiffness on adult neural stem cell behavior. Biomaterials 2009, 30, 6867-6878.
http://dx.doi.org/10.1016/j.biomaterials.2009.09.002
PMid:19775749

36. Schmidt, C. E.; Shastri, V. R.; Vacanti, J. P.; Langer, R., Stimulation of neurite outgrowth using an electrically conducting polymer. Proceedings of the National Academy of Sciences of the United States of America 1997, 94, 8948-8953.
http://dx.doi.org/10.1073/pnas.94.17.8948
PMid:9256415 PMCid:PMC22977

37. Yavin, E.; Yavin, Z., ATTACHMENT AND CULTURE OF DISSOCIATED CELLS FROM RAT EMBRYO CEREBRAL HEMISPHERES ON POLYLYSINE-COATED SURFACE. J. Cell Biol. 1974, 62, 540-546.
http://dx.doi.org/10.1083/jcb.62.2.540
PMid:4609989 PMCid:PMC2109386